Experimental Study of a Planar Expansion-Deflection Nozzle

B. Wagner and R. Stark
German Aerospace Center, Institute of Space Propulsion
Lampoldshausen, 74239 Hardthausen, Germany

Abstract

A planar expansion-deflection nozzle was tested on the cold flow test bench P6.2 at DLR Lampoldshausen. The comparison between experimental data, design, and numerical results at the design point show a good agreement in general with a slight deviation due to a higher expansion in the experiments. The wake closure was investigated on transient pressure profiles. A hysterisis is existing in these experiments for the transition from open to closed operation mode and back. For low pressure ratios in the off design region, flow separation on the center body was observed. The separation shock interacts with the outer contour leading to pressure peaks.

1. Introduction

In the early 1960s research work began on alternative nozzle concepts which were capable to adapt to the ambient pressure. At this time the expansion-deflection (ED) nozzle concept was developed.[9] The ED nozzle seemed to be a promising idea, due to a free boundary inside the nozzle. But due to different reasons, e.g. the altitude compensation was in doubt,[17] an ED nozzle was not further considered for a rocket main engine.
Nowadays, the ED concept is again under consideration to work as upper stage engine.[2] The shorter nozzle length could lead to a mass saving at comparable performance, especially if the combustion chamber is integrated into the nozzle. Thus, the injection direction in the combustion chamber is reverse to the outflow direction at the nozzle exit. Furthermore, expander cycle type engines could benefit from the increased heat transfer at the large surface areas and the shaped throat region, typical the region with the highest heat transfer.[5]
Recently detailed analytical and numerical investigations of the flow behaviour and the performance of an ED nozzle have been made for both atmospherice flight and vacuum conditions.[15] Numerical methods, e.g. for the sonic line evaluation have been combined with the method of characteristics (MOC) for the flowfield calculation.[16] The shape of the sonic line influences the starting line of the MOC and hence the entire nozzle design. The simple analytical investigation for conventional nozzles as e.g. Sauer[10] are not capable for the throat modeling in ED nozzle due inclined throat flow without a clear dominant velocity vector. Numerical approaches to estimate the sonic line seem to be the only practicable way, but the results need experimental validation.
The central body with the viscous flow region at the base is another critical design area. The MOC is limited to the supersonic flow field. Additional methods must be used to predict the base pressure as it has an impact on the overall performance of the nozzle. The transition from open to closed wake mode are also excluded from the MOC design. Computational fluid analysis can support the design process, but for their reliability they need to be validated.
Therefore, an ED nozzle test programm was started a DLR Lampoldshausen to verify the existing design tools and to build a database for CFD validation. The first ED nozzle is planar and has an equal inflow and outflow direction. The critical design areas, the throat and the base area are under investigation with optical diagnostic and pressure measurements. The influence of the extended pintle is of special interest as this represents the integrated combustion chamber into the supersonic flowfield.

2. Flowfield

The flowfield inside an ED nozzle can be devided into two operation modes which depend on the pressure ratio of supply to ambient pressure. At very low ambient pressures or vacuum conditions, thus at high pressure ratios, the nozzle operates in the closed wake mode. The flow expands around the central body, the boundary layer separates and continues as shear layer between the supersonic nozzle flow and the subsonic flow region behind the central body. The flow region at the base is trapped by the shear layer, no connection to the ambient is possible. The shearing forces lead

to a closed recirculation. The supersonic flow deflected by the expansion must be redirected parallel to the centerline. Thus a shock wave is generated while the shear layer turns at the centerline. Under sea level conditions, the closed wake mode can also be obtained by a sufficiently high supply pressure. This is the case for the presented configuration (figure 1a). So the flow is expanded to sea level pressure and the pressure upstream the central body is chosen to expand the flow around the pintle corner towards the centerline.

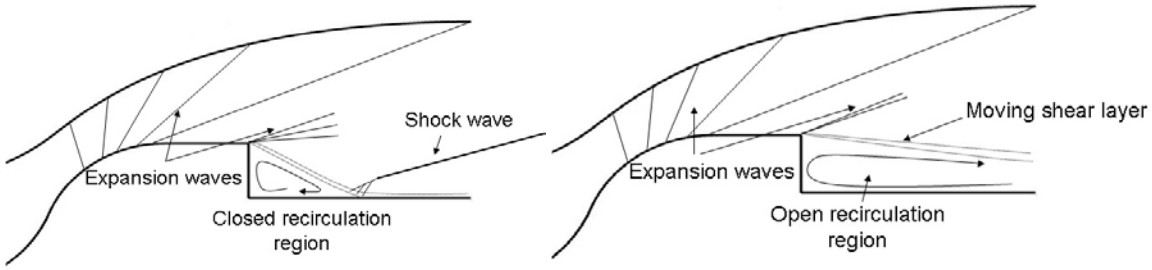

(a) Closed wake mode.

(b) Open wake mode.

Figure 1: Flow features inside the tested ED nozzle

In the case of lower pressure ratios, wake closure is not achieved. The shear layer acts as free boundary between the supersonic flow and the viscous recirculation zone which is connected to the ambient pressure. The shear layer moves towards the centerline with increasing the pressure ratio or vice versa. The aspiration effect of the shear layer is responsible for the pressure at the base which is, therefore, lower than the ambient pressure. This flow behaviour is called open wake mode (figure 1b).

3. Experimental Setup

3.1 Test Bench

The cold gas subscale test facility P6.2[3] at the German Aerospace Center (DLR) in Lampoldshausen was used for the presented experiments. The test bench consists of two test positions, a closed high altitude simulation chamber,[11] and a horizontal test position under ambient conditions. Blow down test against ambient pressure with a maxiumum feeding pressure of 4 MPa were performed (see flow plan figure 2a). The propelling gas, dry nitrogen, is stored in seven high pressure tanks at 20 MPa under ambient conditions. Due to the large massflow during the experiments, all tanks were joined to provide sufficient primary pressure. After passing the hand valves and the automatic valve, the nitrogen is cleaned from small particles in the high pressure filter before entering the pressure regulator. Finally, the test sequenzes are controlled by the fraction of total width of the control valve and have a high accuracy in both nominal values and reproducibility.

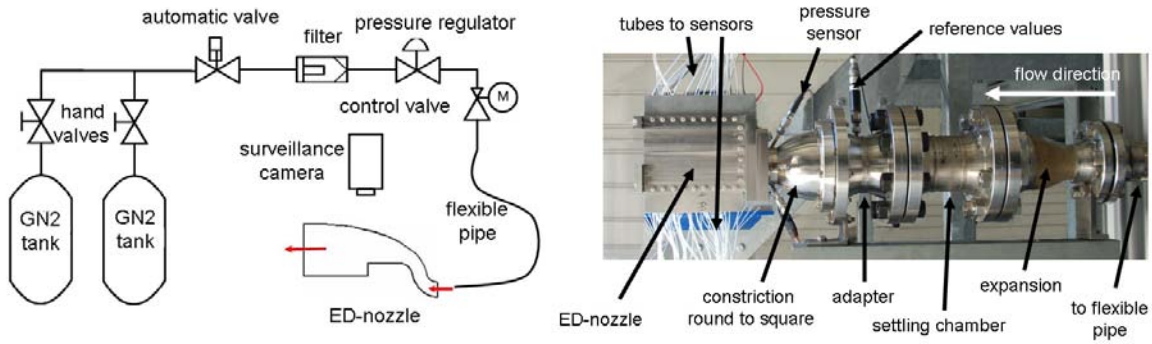

(a) Sketch of the 4 MPa feeding system.

(b) Picture of the horizontal setup. In the background, mounting of the vacuum chamber.

Figure 2: Integration of the experimental setup into P6.2

After the flexible pipe, the flow is expanded to the largest cross section area in the setup, which is $12.8 \cdot A_t$ where A_t is the smallest area located in the nozzle throat. At this location with the lowest flow velocity the settling chamber

is placed. It consists of a honeycome structure of a tubesize of 3.5 mm and three meshes with a mesh size of 2 mm. A plenum is attached to the settling chamber, with the same diameter. The total pressure (p_0) and total temperature are measured in this part (see figure 2b).
The constriction from the large round cross section to the nozzle inlet is carried out simultaneous with the transition from a round to a squared cross section. In order to provide a homogeneous flow field, the constriction contour was designed as wind tunnel constriction proposed by Boerger.[1] This method minimizes the length of a constriction at a given constriction ratio, avoiding flow separation, and leading to a homogeneous flowfield at the exit while using a 5th order equation approach. This component was built from one part by eroding the inner contour with several copper electrodes.

3.2 Nozzle

Although, planar nozzles are unlikely to be used in rocket propulsion, they benefit from a good access for measurement techniques, especially for optical diagnostics, e.g. schlieren visualisation. A drawback of planar setup is the corner flow and the difficulties in manufacturing and sealing. By laser welding the two nozzle parts into the flange frame these problems could be solved, while keeping access to the flow field through removable side walls. Instead of a symmetric nozzle, only one part of an ED nozzle was designed. Thus, this increases the throat area for measurements at a given maximum massflow which is limited by the test bench. The symmetric line, which would normaly be behind the central body is substituted by a solid wall. This part can also be equiped with pressure sensors.
The inflow area is given by the constriction which is a squared cross section with a width of $2.5\,G_t$. G_t is the smallest distance between the upper contour and lower pintle wall. Details of the throat area can be found in figure 3a. The throat design is comparable to the model proposed by Taylor[16] omitting the contour radius downstream G_t and simpler pintle radii shape.

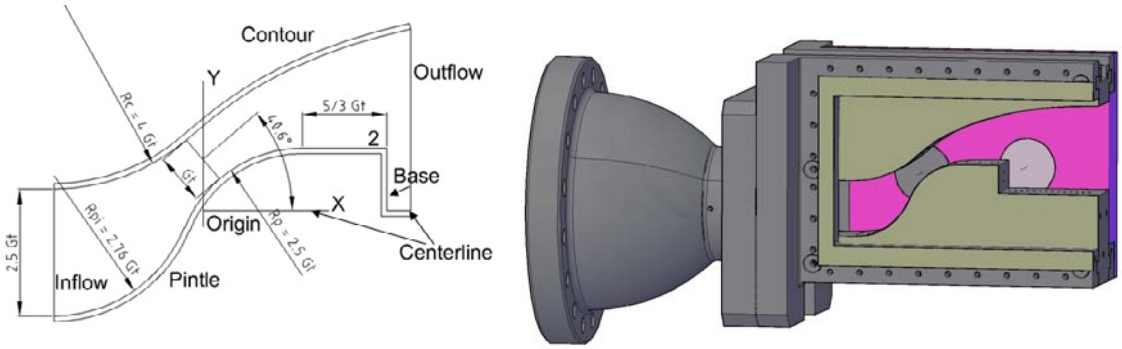

(a) Throat region in detail.

(b) CAD model of the nozzle attached to the constriction. Positions of the schlieren windows are indicated.

Figure 3: Tested planar ED nozzle.

The contour is designed for $p_2/p_a = 1.8$ at the end of the pintle (see position 2 in figure 3a and p_a is the ambient pressure). The pressure ratio was chosen to assure wake closure for $p_0/p_a = 30$ without uncertainties. The actual transition point is part of the experimental investigation. As guideline for the dimensioning, the experiments of Mueller[8] were considered, where wake closure was achieved for $p_2/p_a = 1.63$.
The exit conditions of the nozzle are given by an expansion to the ambient pressure at sea level. The wall contour is designed by a Prandtl-Meyer expansion resulting in an area ratio of 4. With the given boundary conditions, it was not possible to keep the inflow line and the centerline of the pintle on the same level. The X-axes is indentical to the centerline behind the pintle. Its origin is located in the middle of the smallest gap between contour and pintle as it can be seen in figure 3a. The flow direction in the throat is 40.6° inclined to the centerline. As the inflow and the outflow direction are the same, this setup is called linear flow configuration. Two other configurations including a reverse flow nozzle are planned. The throat region was also designed to fit those future configurations.
New at this design is the extended center body. The expansion ends at the downstream radius after the throat, but the pintle was elongated by $5/3 \cdot G_t$ parallel to the centerline where no further expansion takes place. The pintle shape is derived from the design of a reverse flow nozzle with the combustion chamber integrated into the nozzle. This configuration would lead to conical body in the supersonic flow region.[2]

3.3 Data Acquisition

The 0.5 mm pressure orifice are connected with steel tubes, which are laser welded into the outer nozzle walls. Those tubes are joined through a teflon pipe with an interface block in which the pressure sensors are mounted. To ease the mounting of the setup, the pipes are chained with Quick-Disconnects. 34 pressure sensors in the range of 0.07 MPa to 5 MPa are used, mostly Kulite (XT-154-190M) and some Kistler (4043) sensors.
The signal of the pressure sensors is amplified and filtered with a low-pass cut-off frequency of 160 Hz in inhouse developed AS2 amplifiers. The data is stored with a sampling rate of 1kHz. For the following test campaigns high frequency channels can also be used with the sampling rate up to 100 kHz.
The pressure sensors were calibrated statically prior the campaign. An offset correction was done before each test run relative to the ambient pressure.

3.4 Test Profile

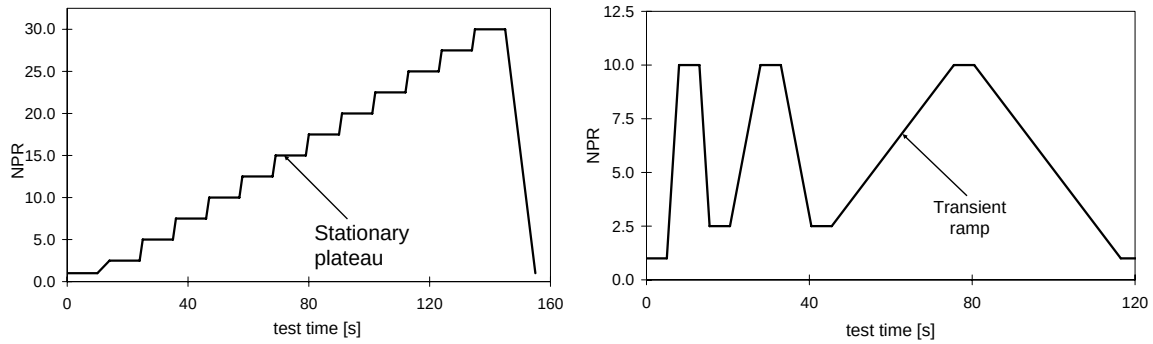

(a) Profile with stationary plateaus.

(b) Profile with transient ramps.

Figure 4: Examples of test profiles

Three main types of supply pressure profiles were considered, from which the test sequences have been derived. Each typ of profile covers a different flow feature of the ED nozzle. For an easier comparison the nozzle pressure ratio (NPR) is used for the ratio of supply to ambient pressure (p_0/p_a). The first profile was an upramping profile with stationary plateaus each NPR = 2.5 steps (figure 4a). On the plateaus mean values could be built of the data and stationary wall and base pressure distributions were gained. Up- and downramping with different gradients in the transition region (NPR = 15 – 25) was the objective of the second main test configuration. With this profile the wake closure should be deteremined. The third profile varies the supply pressure in the low pressure region NPR = 2.5 – 10 as the flow behaviour at the off design is of interest (figure 4b). Due to the lower wall pressures the sensors could be redistributed along the nozzle surfaces.

4. Results

4.1 General Flow Behaviour

The data of the plateau experiments can be compared to the design values. CFD calculations were performed according to the experimental total conditions and they are also compared. The DLR TAU code[6] was used for the numerical simulations. The Reynolds averaged Navier-Stokes equations were solved on a quasi two dimensional hybrid mesh. The full turbulent flow was computed with the Spalart-Allmaras model due to previous good experiences with this model[12,13] for nozzle flows. Local grid refinement was used for a higher resolution of the flowfield inside and shortly downstream the nozzle. Around the nozzle a farefield boundary with ambient conditions was used. The y^+ at the adiabatic walls is around 1.

The experimental values are taken during stationary flow on pressure plateaus and are averaged over a minimum of one second. The values are normalised by the total condition. In figure 5a the pintle shape is additionally plotted. In the convex part of the pintle, the pressure decrases rapidly, because the flow is expanded and therefore accelerated along the wall. The accelaration ends at the linear part of the center body, hence no further pressure decrease is existing. Both the numerical and the experimental date show a lower pressure distribution than the design especially on the center body. Either the expansion along the pintle is underpredicted in the design or the dismatch of the assumed to the

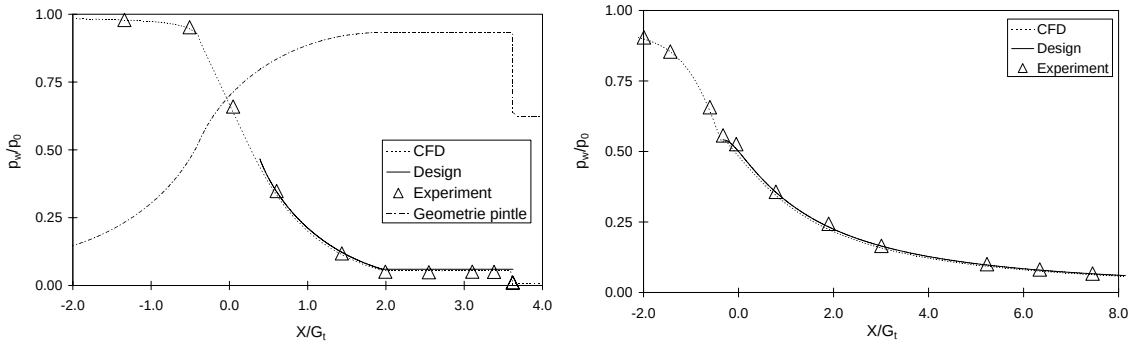

(a) Pintle. (b) Contour.

Figure 5: Comparision CFD, experiment, and design.

actually sonic line leds to an additional expansion which could emanated from the contour side.
In figure 5b the comparision is carried out for the contour side. In general a good agreement can be found, but again the numerical results show a slightly higher expansion along the contour. The small delay in the expansion at the intersection of wall radius and contour profile indicate a weakness in the design for those intersections and will be improved.
The incoming pressure on the contour side (at the axial position $X/G_t = -2.0$) is lower then the pintle one. Due to the pintle shape the flow is delayed in the concave part as on the contour side it is continously accelerated.

4.2 Base Pressure and Flow Transition

The pressure at the pintle base (p_b) was measured statically at two positions with a distance of $0.41 \cdot G_t$ and $0.81 \cdot G_t$ from the centerline, respectively. The difference between these two gauges is within the measurement uncertainties, thus p_b is presented as the meanvalue of both sensors.
With the plateau test profiles expierence about the flow transition was gained at stationary conditions and with a coarse resolution. According to figure 6a the transition between open and closed operation mode takes place between NPR 20 and 23.2. Increasing the NPR the pressure at the base is decreasing as the result of the aspiration effect of the recirculation zone. The shear layer turns to the centerline due to the expansion around the pintle corner. Thus, the supersonic flow region widens as the pressure rises, but the recirculation zone behind the pintle becomes, therefore, smaller, the recirculating flow is accelerated, the aspirations effect is intensified and the base pressure reduces. At the closed operation mode the recirculation zone becomes a trapped vortex. The connection to the ambient is cut. The pressure of this vortex is now only linked to the superconic flow. Thus, the base pressure also increases with further rise of the NPR.
A more detailed view of the transition process is give by the plot of the base pressure distribution during a single up- and downramping in figure 6a. Like in the stationary results the base pressure decrases with higher NPRs. It showes a steeper gradient then the supply pressure just in front of the transition. The actual transition is characterised by decreas of 2/3 of the base pressure within 50 ms. At higher NPRs the base pressure increases as it is not connected to the ambient anymore and the aspiration effect is omitted. The base region, with the trapped vortex is further only compressed by the supersonic expanding around the base corner.
On the downramping profil, thus if the NPR has a negative gradient, the behaviour of the base pressure differs from the upramping. The derivation occurs from the transition point at around NPR = 21.8 on. At this point the minimum base pressure of $p_b/p_a = 0.25$ is reached. But with further lowering of the NPR it is increasing again. Even a small jump of $\triangle p_b/p_a = 0.05$ at around NPR = 21.25 can be found. This first aberration is present in all base pressure distributions, but the shape is not always that strong as in the shown profile. After this small pressure rise the base pressure acts like in the open wake mode, because the base pressure reacts contrarian to the NPR. The retransition takes place at a NPR = 18.2, also with a duration of 50 ms. The base pressure jumps back to the pressure value of the open mode. It is interesting to note that the pressure downstream of the redirection shock wave (see figure 1a) does not show this behaviour. It further decreases until the retransition point. Thus, on a downramping profile, the situation between the transition and retransition point cannot be described with the flow feature of a closed operation mode due to the contrarian behaviour of the base pressure. The obvious hysteresis effect needs further investigation on the effect of condensation as it was observed by Mueller[7] and on the effect of the wall at the centerline which substitutes the symmetric line.

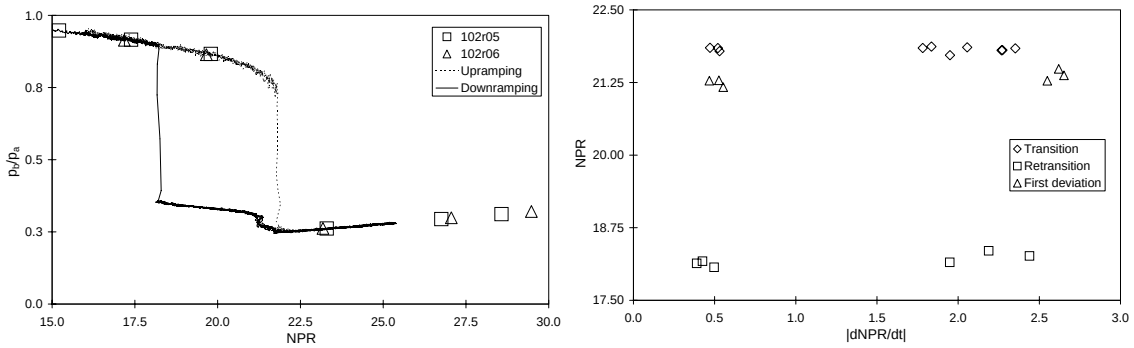

(a) Base pressure distribution, open to close transition.

(b) Transition behaviour for different NPR gradients.

Figure 6: Open to close mode transition.

In figure 6b the transition and retransition points are shown. The NPR is plotted versus the absolut gradient of the NPR. The number of transition experiments exceeds the number of retransitions, because data from the plateau profil tests was also used. For those test the retransition occured during the shut down process and proper test conditions cannot be assured. All data was taken at the beginning of the sudden change in the pressure distribution. As mentioned before, the transition takes around 50 ms. However, both the transition and the retransition data show a very small difference between the test runs. Additional, no influence of the ramping gradient, the change rate of NPR could be found.
The first deviation, so the first sudden pressure rise without retransition in the base pressure profile on a decreasing NPR gradient is indicated by the triangles. It occurs at a NPR = 21.25 with a tendency to begin at a slightly higher pressure ratios for larger gradients.

4.3 Off Design Flow

Although, the area of application of nowadays ED nozzles would be in an upper stage engine or on a moon/planet soft landing mission, which means almost or full vacuum conditions at the exit, an understanding of the flow field at very low pressure ratios is needed for ground testing. As the first experiments of a scaled ED nozzles would be at test facilities working under ambient conditions. Under these conditions very low NPRs are passed during the transient start-up and shut-down processes and the flowfield features behaviour far from the design point. Those flow features could include separation, causing side loads and undesirable shock interaction.
Therefore, tests in the off design were performed, varying the NPR between 2.5 and 10 with different gradients. Under

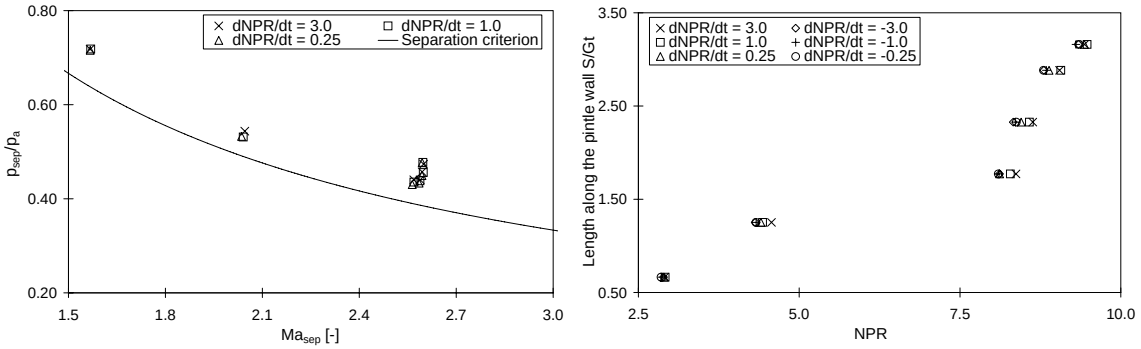

(a) Separation positions on the pintle compared to criterion of Stark.

(b) Separation positions along the pintle wall.

Figure 7: Flow separation at low NPRs.

this test conditions flow separation was observed on the pintle. In figure 7a the position of the separation is plotted versus the resulting Mach number (Ma_{sep}) for the separation pressure (p_{sep}). The separation could only be determined by the sudden change in the pressure distribution caused by the moving separation front. Thus the date is limited to sensor positions. Separation data is presented for clarity only on upramping profiles but for different NPR gradients and has been averaged over several tests. The concentration of points at $Ma_{sep} = 2.6$ is related to the sensors on the straight pintle wall where the flow is not further accelareted, but the movement of the separation front along this wall

can still be measured.
Included in figure 7a is the criterion suggest by Stark,[14] where $p_{sep}/p_a = 1/Ma_{sep}$, and that is valid for turbulent separation in bell type nozzles. The data shows comparatively higher separation pressures, like it can be found for planar nozzles in literature.[4]
Figure 7b clarifies the movement of the separation along the pintle wall. The separation position is plotted for the actual length along the contour. At the transition of pintle radius to straight pintle the third pressure orifice is located ($1.7 \cdot S/G_t$). The separation must be delayed just in front of this position, since a large gap in the separation profile between NPR = 4.5 and NPR = 8.0 is existing. Furthermore, the transition from laminar to turbulent separation might be indicated by the offset of the $1.7 \cdot S/G_t$ orifice data to the linear behaviour of the subsequent gauges.
The separation which occurs along the pintle wall generates a separation shock. This causes a flow interaction at the contour which is visable in the wall pressure distribution in figure 8. The wall pressure is normalized by the ambient pressure and is plotted along the contour length for different NPRs. The array of curves have an offset according to the NPR in the undisturbed region. The discrepancy from the vacuum profile takes place depending on the NPR around $p_w/p_a = 1.0$ for low NPR, down to $p_w/p_a = 0.7$ for higher NPRs. The flow is recompressed at the contour probably by the interaction with the separation shock coming from the pintle. The interaction could either be an ordinary shock reflection or shock reflection with a separated zone. This effect will be further investigated. Note that the contour pressure is recompressed up to $p_w/p_a = 2.0$ for NPR = 5.0 e.g., but expands to 1.1 of the ambient pressure at the nozzle exit. For NPR = 7.0 no expansion after the pressure rise is visible, because it is too close to the nozzle end. As the exit pressure is always above the ambient pressure normal flow separation can be excluded, because in this case the region behind the separation shock would be dominated by the ambient pressure. For NPR = 10.0 no discrepancy from the vacuum profile can be found anymore. This is according to the findings of figure 7b that the last measured separation occurs for NPR around 9.

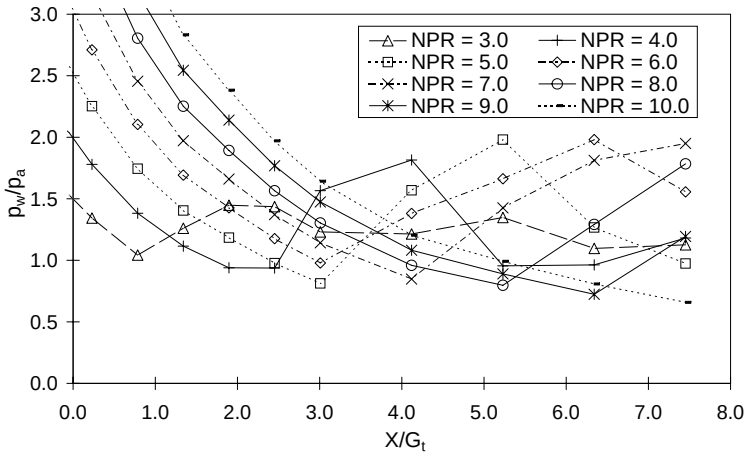

Figure 8: Pressure distribution along the nozzle contour for low NPRs.

5. Summary and Outlook

A planar ED nozzle was tested at the cold flow test bench P6.2. Experiments at the design point and off design were performed. The transition between open and closed mode was observed and a hysteresis effect is found. On decreasing NPRs the base pressure behaves contrarian to the expected further expansion. At very low NPRs flow separation occurs on the pintle. The separation is delayed at the end of the convex pintle part and moves along the linear part. The separation behaviour is independent from the the NPR gradient. Accompanying numerical simulations are ongoing and will be validated with the experimental results.
The presented experiments are part of the ED test programm at DLR Lampoldshausen. The next step are tests with optical diagnostic through the window segments. The throat and the base region are of interest, nevertheless the whole flowfield will be observed. The wake closure and opening will be investigated in more detail as additional sidewall pressure measurements will be done.
Future tests at the test bench M11 are planned. An air heater will be used to provide hot humid air up to 1300 K for further temperature depended investigations. The nozzle will then be equipped with thermocouples around the throat region.

Acknowledgment

The test bench was operated by C. Boehm, his help and support is appreciated.

References

[1] Boerger G. Optimierung von Windkanalduesen fuer den Unterschallbereich. PhD thesis, Fakultaet fuer Maschinenbau und Konstruktiven Ingenieurbau, Ruhr-Universitaet Bochum, 1973.

[2] Goetz A., Hagemann G., Kretschmer J., Schwane R. Advanced upper stage propulsion concept - the expansion-deflection upper stage. In *41st Joint Propulsion Conference*, AIAA 2005-3752, Tuscon, 2005.

[3] Kronmueller H. and Schaefer K. Cold gas subscale test facility P6.2 at DLR Lampoldshausen. In *6th International Symposium for Space Transportation of the XX1 st Century*, Versailles, 2002.

[4] Lawrence R. Symmetrical and unsymmetrical flow separation in supersonic nozzles. Institute of Technology of Southern Methodist University, PhD Thesis, NASA CR 92587, 1967.

[5] Lentsch A. and Leudiere V. Performace estimation of an expander bleed cycle. In *4th International Conference on Laucher Technology*, Liege, 2002.

[6] Mack A. and Hannemann V. Validation of the unstructured DLR-TAU-code for hypersonic flows. In *32nd Fluid Dynamics Conference and Exhibit*, AIAA 2002-3111, St. Louis, 2002.

[7] Mueller T. and Hall C. On the separated flow region within a planar expansion-deflection nozzle. In *6th Aerospace Sciences Meeting*, AIAA 68-82, New York, 1968.

[8] Mueller T. and Hall C. Separated flow region within a planar expansion-deflection nozzle. *Journal of Spacecraft*, 5, 738–740, 1968.

[9] Rao G. The E-D nozzle. *Astronautics*, 28–29,50–51, 1960.

[10] Sauer, S. General characteristics of the flow through nozzles at near critical speeds. NACA TM-1147, reprint 1947.

[11] Schaefer K., Boehm C., Kronmueller H., Stark R., Zimmermann H. P6.2 cold gas test facility for simulation of flight conditions - current activities. In *1st European Conference for Aerospace Sciences*, Moscow, 2005.

[12] Stark R. and Wagner B. Experimental flow investigation of a truncated ideal contour nozzle. In *42nd Joint Propulsion Conference*, AIAA 2006-5208, Sacramento, 2006.

[13] Stark R. and Hagemann G. Current status of numerical flow prediction for separated nozzle flows. In *2nd European Conference for Aerospace Sciences*, Brussel, 2007.

[14] Stark R. and Wagner B. Experimental study of boundary layer separation in truncated ideal contour nozzles. *Shock Waves*, 19, 185–191, 2009.

[15] Taylor N. An integrated approach to expansion deflection nozzle analysis. PhD thesis, University of Bristol, 2002.

[16] Taylor N. and Hempsell C. Throat flow modelling of expansion deflection nozzles. *Journal of the British Interplanetary Society*, 57, 242–250, 2004.

[17] Wasko R. Performance of annular plug and expansion-deflection nozzles including external flow effects at transonic Mach numbers. NASA TN D-4462, 1968.